

SCIENTIFIC REPORTS

OPEN

Compositional marker *in vivo* reveals intramyocellular lipid turnover during fasting-induced lipolysis

Ajay Thankamony¹, Graham J. Kemp², Albert Koulman^{3,4}, Vlada Bokii⁵, David B. Savage⁴, Chris Boesch⁶, Leanne Hodson⁷, David B. Dunger^{1,4} & Alison Sleigh^{4,5,8}

Intramyocellular lipid (IMCL) is of particular metabolic interest, but despite many proton magnetic resonance spectroscopy (¹H MRS) studies reporting IMCL content measured by the methylene (CH₂) resonance signal, little is known about its composition. Here we validated IMCL CH₃:CH₂ ratio as a compositional marker using ¹H MRS at short echo time, and investigated IMCL content and composition during a 28-hour fast in 24 healthy males. Increases in IMCL CH₂ relative to the creatine and phosphocreatine resonance (Cr) at 3.0 ppm (an internal standard) correlated with circulating free fatty acid (FA) concentrations, supporting the concept of increased FA influx into IMCL. Significant decreases in IMCL CH₃:CH₂ ratio indicated a less unsaturated IMCL pool after fasting, and this compositional change related inversely to IMCL baseline composition, suggesting a selective efflux of unsaturated shorter-chain FA from the IMCL pool. This novel *in vivo* evidence reveals IMCL turnover during extended fasting, consistent with the concept of a flexible, responsive myocellular lipid store. There were also differences between soleus and tibialis anterior in basal IMCL composition and in response to fasting. We discuss the potential of this marker for providing insights into normal physiology and mechanisms of disease.

Intramyocellular lipids (IMCL) assemble as tiny droplets close to mitochondria and are dynamic functional organelles involved in lipid metabolism and cell signalling^{1,2}. Associated with enzymes of fatty acid (FA) esterification, hydrolysis and mitochondrial transport, they represent a metabolically active pool optimised for rapid FA turnover and oxidation. IMCL accumulation is associated with insulin resistance (IR)^{3–5}, but the occurrence of increased IMCL also in states of high insulin sensitivity (the ‘athlete’s paradox’)⁶ has focused attention on related lipid intermediates (e.g. ceramide, diacylglycerol or long-chain fatty acyl CoA), rather than intramyocellular triglyceride (TG) *per se*, in impaired insulin signalling².

Fasting-induced adipose tissue lipolysis releases free fatty acids (FFA) into circulation and IMCL are reported to increase^{7,8}, in a fibre-specific manner^{8–11}. This suggests that the relationship between FA availability and oxidation, rather than circulating insulin, mainly determines IMCL content⁷. In fasting, both highly unsaturated FA and shorter-chained FA are preferentially mobilised from adipose tissue^{12,13}, and a similar pattern is evident from changes in biopsy-measured rat muscle TG during an extended fast¹⁴. The mechanism for this preferential mobilisation was thought to relate to the physico-chemical characteristics of individual fatty acids^{12,13}, such as water solubility, but selective enzymological properties were not ruled out¹⁵.

¹Department of Paediatrics, University of Cambridge, Cambridge, UK. ²Department of Musculoskeletal Biology, University of Liverpool and MRC–Arthritis Research UK Centre for Integrated research into Musculoskeletal Ageing (CIMA), Liverpool, UK. ³National Institute for Health Research Biomedical Research Centre (NIHR BRC) Core Metabolomics and Lipidomics Laboratory, University of Cambridge, Cambridge, UK. ⁴Wellcome Trust–MRC Institute of Metabolic Science, Cambridge, UK. ⁵Wolfson Brain Imaging Centre, University of Cambridge School of Clinical Medicine, Cambridge, UK. ⁶Department of Clinical Research and Radiology, AMSM, University Bern, Bern, Switzerland. ⁷Oxford Centre for Diabetes, Endocrinology and Metabolism (OCDEM), Radcliffe Department of Medicine, University of Oxford, Oxford, UK. ⁸National Institute for Health Research/Wellcome Trust Clinical Research Facility, Cambridge University Hospitals NHS Foundation Trust, Cambridge, UK. Correspondence and requests for materials should be addressed to A.S. (email: as626@wbic.cam.ac.uk)

The unique ability of proton magnetic resonance spectroscopy (^1H MRS) to non-invasively distinguish IMCL from extramyocellular lipid (EMCL)^{16,17} has led to its widespread use, reporting IMCL concentrations from the signal intensity of the methylene (CH_2) resonance in FA chains in TG (the predominant species detected by ^1H MRS¹⁸). However, CH_2 signal is also influenced by lipid composition, a notional normal value being assumed to quantify IMCL. In contrast, the methyl (CH_3) resonance is independent of lipid composition¹⁸, but measurement is hampered by its lower signal intensity and the overlapping EMCL CH_3 resonance. To address this Ren *et al.*¹⁹ exploited the spectral simplification of long echo time acquisition and the enhanced signal-to-noise and spectral resolution at 7 T. They proposed the $\text{CH}_3:\text{CH}_2$ ratio as a marker of IMCL TG composition¹⁹. However, at long echo times the reduction in signal and the need for accurate T_2 correction^{19,20} pose challenges, and its practical utility has not been established.

Most muscle IMCL measurements are made at 3 T with a short echo time. We set out to test the feasibility of measuring the CH_3 resonance under these conditions, using optimal quality spectra and fitting algorithms. To evaluate the $\text{CH}_3:\text{CH}_2$ ratio as a compositional marker, we measured it *in vitro* in phantoms simulating IMCL and EMCL. To study IMCL composition and dynamics during extended fasting we performed ^1H MRS at short echo time in healthy males at both 8 h (a standard baseline time point for metabolic studies regarding food intake) and 28 h of fast. We measured *in vivo* changes in CH_2 (influenced both by TG amount and composition), CH_3 (reporting only TG amount, and thus reflecting net FA influx-efflux) and $\text{CH}_3:\text{CH}_2$ (the compositional marker) in two leg muscles, the more oxidative soleus (SOL) and the more glycolytic tibialis anterior (TA), and related these to circulating FFA concentrations and changes in MRI-measured adipose tissue volumes.

Results and Discussion

Phantom validation. The IMCL $\text{CH}_3:\text{CH}_2$ ratio is sensitive to unsaturation, and to a lesser degree the chain length in intramyocellular TG (Fig. 1A). In agar phantoms simulating the combined IMCL and EMCL pools, the $\text{CH}_3:\text{CH}_2$ ratio correctly distinguished 4 different lipid compositions by their relative order (Fig. 1B, right). Bias due to factors including J-modulation, fitting prior knowledge, and T_2 effects likely account for the systematic difference between observed and theoretical values, so ratio values were used comparatively. Figure 1B and C show representative spectra (and the corresponding fits) acquired from a phantom and from SOL *in vivo*, respectively. The CH_3 signal from omega-3 FA resonates at different frequencies to the CH_3 resonance shown in Fig. 1, but as shown by biopsy, muscle TG contains very little (~1%) omega-3 lipids²¹ and so the fitting models we used disregard this.

***In vivo* fasting effects.** The 24 healthy male participants were of mean \pm SEM age 34.9 ± 1.8 years and BMI $23.4 \pm 0.5 \text{ kg}\cdot\text{m}^{-2}$. Spectra with no clear distinction between EMCL and IMCL CH_2 resonances were eliminated, yielding 22 and 19 complete pre- and post-fasting sets for TA and SOL respectively. IMCL CH_2 relative to the internal standard creatine plus phosphocreatine (Cr) increased on extended fasting (Table 1), consistent with observations in longer fasts in human vastus lateralis⁷, TA and SOL⁸. FFA concentrations correlated with the fasting increment (Δ) in IMCL in both TA (ΔCH_2 : $r = 0.57$, $p = 0.006$; ΔCH_3 : $r = 0.39$, $p = 0.07$) and SOL (ΔCH_2 : $r = 0.52$, $p = 0.02$; ΔCH_3 : $r = 0.47$, $p = 0.04$), supporting the concept that FA influx into the cell controls IMCL pool size in these circumstances, either by directly altering the influx into the IMCL pool or indirectly by suppressing IMCL lipolysis. Subcutaneous adipose tissue (SCAT) decreased whilst other fat depots remained unchanged (Table 1), suggesting that SCAT is the main source of increased FFA in these non-obese males. This is consistent with studies of regional FFA release *in vivo* in humans using isotope techniques²² where upper body subcutaneous fat was by far the greatest contributor to systemic FFA release under basal conditions and during prolonged fasting. Direct validation studies would be needed to support this application of MRI in determining the dynamics of fat depots conveniently *in vivo*.

IMCL CH_3/Cr (which unlike CH_2/Cr , the increment in which purely reflects net FA flux) increased by ~12% in TA ($p = 0.03$) implying net FA influx during the fast, but not significantly in SOL. IMCL CH_2/Cr increased by 26% in SOL ($p = 0.007$) and 31% in TA ($p < 0.001$) (Table 1). The IMCL CH_2/Cr increase was therefore more than the increase in CH_3/Cr and thus represents significant decreases in the compositional marker $\text{CH}_3:\text{CH}_2$ (Table 1, Fig. 2A), indicating a change towards decreased unsaturation and possibly increased chain length of IMCL during fasting. These IMCL compositional changes on fasting correlated inversely with baseline IMCL composition in both muscles (Fig. 2A), suggesting a selective efflux of unsaturated and/or shorter chain FAs from the IMCL pool during fasting. This matches the mobilisation profile in a rat biopsy study of muscle TG¹⁴, in which the reduction in $\text{CH}_3:\text{CH}_2$ ratio was mainly due to the efflux of unsaturated and/or shorter chain FA. Supporting this notion, net efflux of FFA from the IMCL pool during the fast were associated with decreases in the compositional marker in both muscles (Fig. 2B). IMCL compositional changes were not associated with circulating FFA or IMCL $\Delta\text{CH}_2/\text{Cr}$ in either muscle (all $p > 0.23$). Together our observations indicate that during the fast an efflux of FA with a high $\text{CH}_3:\text{CH}_2$ ratio from the IMCL pool is the main determinant of compositional changes in IMCL.

Differences between muscles. There was a striking difference in baseline IMCL $\text{CH}_3:\text{CH}_2$ between muscles (Table 1, Fig. 2C), TA having a more unsaturated shorter-chain TG pool than SOL. Modelling based on phantom results suggests that SOL lipid $\text{CH}_3:\text{CH}_2$ is similar to or more saturated than olive oil, and TA similar to sunflower oil. A possible contribution to these differences may result from inconsistencies in spectral fitting between muscles due to slightly different EMCL resonant frequencies that depend on fibre orientations; however, this is unlikely to fully explain these differences. Biopsy TG samples processed by normal methods are prone to EMCL contamination, and there is little published data on the composition in these muscles; we cautiously suggest that such a difference in IMCL composition might explain reported differences in determinants of IMCL²³.

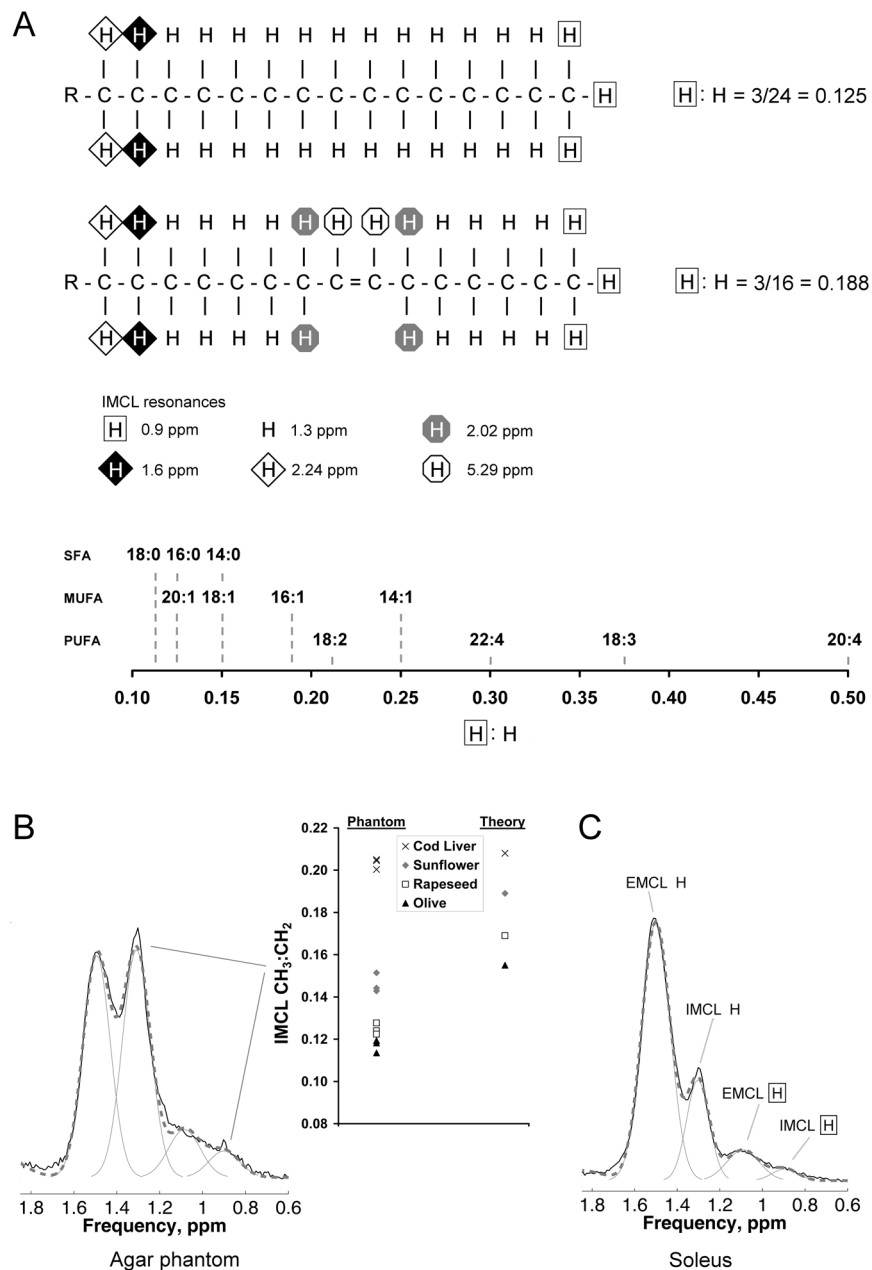


Figure 1. ^1H -MRS intramyocellular lipid (IMCL): the $\text{CH}_3:\text{CH}_2$ ratio as a compositional marker in theory, in phantoms, and *in vivo*. **(A) Theory.** The figure shows the principle of the $\text{CH}_3:\text{CH}_2$ ratio as a compositional marker in IMCL (which detected by ^1H MRS is overwhelmingly triglyceride (TG)³⁴), influenced primarily by the degree of fatty acid (FA) unsaturation, and secondarily by FA chain length. The *upper panel* shows the palmitic acid component of a TG molecule with the theoretical ratio of $3/24 = 0.125$ of CH_3 (at 0.9 ppm) to CH_2 (at 1.3 ppm). The *middle panel* shows how introduction of a single double bond increases this ratio to $3/16 = 0.188$, due not only to the desaturation of two CH_2 , but also to the alteration in the chemical environment of the neighbouring CH_2 . For FA chains of equal number of double bonds, the $\text{CH}_3:\text{CH}_2$ ratio will also be scaled by chain length, although this will have a proportionally smaller effect (*lower panel*). SFA, saturated FA; MUFA, monounsaturated FA; PUFA, polyunsaturated FA. **(B) Results in phantoms.** The graph on the *right of the panel* shows data from agar phantoms simulating IMCL (oil droplets) and extramyocellular lipid (EMCL; oil-soaked tissue roll) made using olive, rapeseed, sunflower and cod liver oils. Three ^1H spectra were acquired from each phantom and the IMCL $\text{CH}_3:\text{CH}_2$ ratio correctly distinguished the order of four oil phantoms. On the *left of the panel* is a representative ^1H spectrum (solid black) acquired from a voxel containing both simulated IMCL and EMCL compartments, also showing the overall fit (dashed grey) and individual fit components (solid grey). **(C) Results *in vivo*.** The figure shows a representative ^1H spectrum from soleus *in vivo*, showing the fit to EMCL and IMCL CH_2 and CH_3 resonances.

	8 h	28 h	P value
Intra- and extramyocellular lipid			
<i>Soleus</i>			
SOL IMCL CH ₂ /Cr	8.5 ± 1.0	10.7 ± 0.9	0.007
SOL IMCL CH ₃ /Cr	1.02 ± 0.12	1.14 ± 0.11	0.243
SOL IMCL CH ₃ :CH ₂	0.118 ± 0.004	0.106 ± 0.004	0.015
SOL EMCL CH ₂ /Cr	16.3 ± 2.3	16.6 ± 1.8	0.735
<i>Tibialis anterior</i>			
TA IMCL CH ₂ /Cr	4.2 ± 0.4	5.5 ± 0.4	< 0.001
TA IMCL CH ₃ /Cr	0.77 ± 0.09	0.86 ± 0.07	0.033
TA IMCL CH ₃ :CH ₂	0.182 ± 0.011	0.157 ± 0.008	0.011
TA EMCL CH ₂ /Cr	10.2 ± 1.2	12.2 ± 1.6	0.157
Adipose tissue			
SCAT _{abd} , cm ³	781 ± 86	758 ± 81	0.012
VAT, cm ³	336 ± 67	335 ± 69	0.650
SCAT _{leg} , cm ²	13.1 ± 1.0	12.7 ± 1.0	0.001
IMF, cm ²	2.4 ± 0.3	2.5 ± 0.2	0.274
Hepatic lipid			
IHL CH ₂ /water, %	0.91 ± 0.2	0.93 ± 0.2	0.082

Table 1. Magnetic resonance measures at 8 h and 28 h of fasting. Data are mean ± SEM. Bold P values are statistically significant ($p < 0.05$), determined by a 2-tailed paired-samples t-test. IMCL, intramyocellular lipid; EMCL, extramyocellular lipid; SOL, soleus; TA, tibialis anterior; CH₂/Cr, CH₂ lipid expressed relative to the chosen internal standard creatine plus phosphocreatine (Cr); CH₃/Cr, CH₃ lipid expressed relative to Cr; CH₃:CH₂, CH₃ lipid relative to CH₂ lipid, used here as a marker of unsaturation; SCAT_{abd}, abdominal subcutaneous adipose tissue; VAT, visceral adipose tissue; SCAT_{leg}, leg subcutaneous adipose tissue; IMF, intermuscular fat; IHL, intrahepatic lipid. $n = 19$ and 22 in SOL and TA respectively.

The two muscles also responded differently to fasting. The increment in SOL correlated with concentrations of combined saturated 14:0 and 16:0 FA, and of 16:0 alone (Fig. 3C), and appeared unrelated ($p > 0.4$) to mono-unsaturated (MUFA) or polyunsaturated fatty acids (PUFA). This agrees with rat biopsy observations of soleus TG after 48 h fast where only 16:0 and 18:0 FA increased¹⁴. By contrast the increment in TA CH₂/Cr was strongly related to circulating MUFA ($p < 0.003$), with a tendency for PUFA ($p = 0.06$), and not related to any individual or combined saturated FA ($p > 0.3$). Figure 3B shows the correlation with oleic acid concentration, the main circulating MUFA²⁴. This suggests a differing net uptake of FA into IMCL during fasting, with the influx of FA with a higher CH₃:CH₂ ratio into the TA muscle IMCL pool, this is a profile which matches the baseline composition. It is unknown whether this differing uptake is a result of selective FA transporters or of a differing FA profile remaining after short-chain and unsaturated FA are preferentially oxidised^{13,25}.

Summary and implications. We have shown by practical validation in IMCL/EMCL simulated phantoms, that the IMCL CH₃:CH₂ ratio in good-quality spectra showing clear distinction between EMCL and IMCL CH₂ resonances, acquired at 3 T using the PRESS sequence with a short echo time of 35 ms is a comparative marker of TG composition. These acquisition parameters are commonly used, and therefore this method has potential for widespread use. Although this marker does not distinguish saturated from mono- or poly-unsaturated FA components of TG, as recently achieved using a specialised sequence²⁶, it is particularly sensitive to differences in the degree of unsaturation and chain length. We stimulated lipolysis using an extended fast in healthy adult males and showed evidence of IMCL turnover, such that IMCL is synthesized from circulating FFA and hydrolysed causing a selective efflux of unsaturated and/or shorter chain FA. This combination of *in vivo* MRS measurements of IMCL CH₂, CH₃ and CH₃:CH₂ with measurements of plasma FFA has the potential to inform on both the composition and net dynamics of this metabolically-active pool. Although isotopic tracer studies such as pulse-chase approaches performed *in vivo*²⁷ may provide more definitive mechanistic information underlying the turnover of a specific FA species in intramuscular triglyceride, ¹H MRS offers the ability to detect the intramyocellular triglyceride pool non-invasively, allowing repeated measures from the same sample conveniently in a timeframe of a few minutes, permitting investigation of net changes of all FA species both within short-term and over longitudinal intervention studies. The ¹H MRS method outlined here, together with isotopic tracer studies, have the potential to better define the involvement of IMCL in insulin-resistant states and their treatments.

Methods

Phantom validation of IMCL compositional marker. Four agar phantoms simulating IMCL (oil droplets) and EMCL (oil-soaked tissue roll)¹⁹ were made using lipids of differing fatty acid (FA) compositions *viz.* olive, rapeseed, sunflower and cod liver oils. These are composed of triglycerides which, on average, increase in degree of unsaturation from predominantly 18:1 (olive) to predominantly 18:2 (sunflower), to a mixture of highly unsaturated and shorter-chain FA (cod liver oil). The same oil was used in both droplet and tissue roll

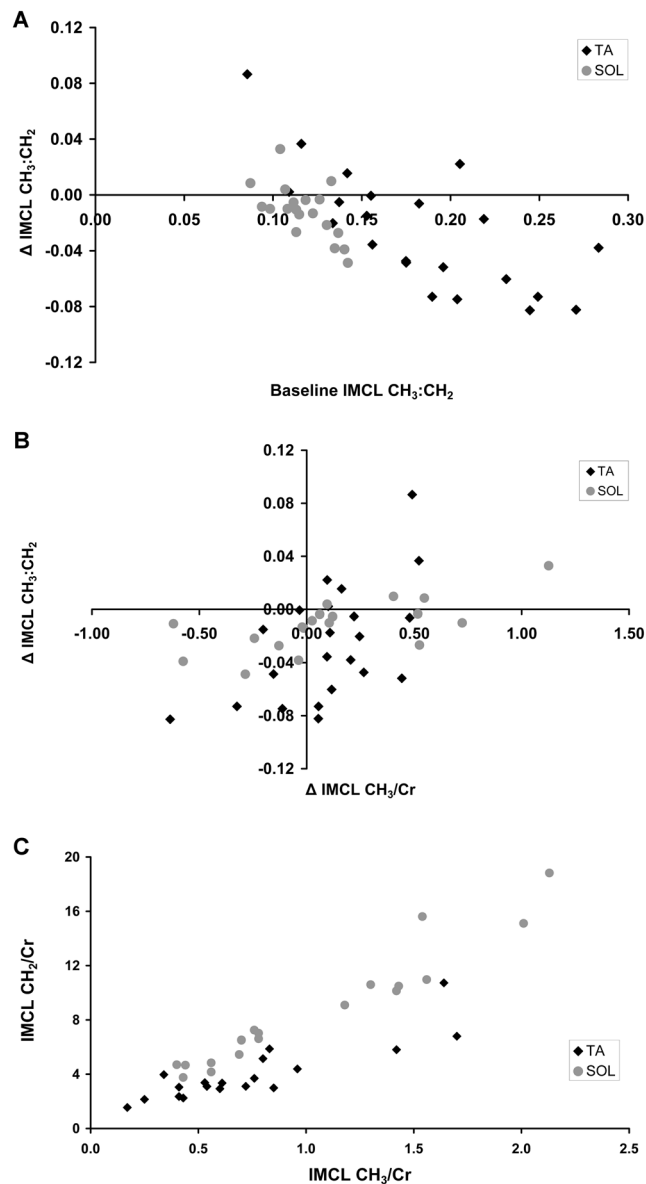


Figure 2. *In vivo* IMCL compositional marker at baseline (8 h fasting) and alterations after extended fasting (28 h) in both the tibialis anterior (TA) and soleus (SOL) muscles. The IMCL CH₃:CH₂ ratio is a marker of the degree of unsaturation combined with reduced chain length. (A) Fasting compositional changes in IMCL relate to the baseline composition. Correlations in the TA (black diamonds; Pearson's $r = -0.73$, $p < 0.001$, $n = 22$) and SOL (grey circles; $r = -0.63$, $p = 0.004$, $n = 19$) muscles, and TA and SOL together ($r = -0.67$, $p < 0.001$, $n = 41$). The overall Δ IMCL CH₃:CH₂ significantly decreased in both muscles during the fast (both $p < 0.015$; paired samples t-test, Table 1). Due to the short TE, T₂ correction would be minimal (estimated to alter CH₃:CH₂ values by ~10%), and is not shown. (B) Fasting compositional changes in IMCL relate to fasting alterations in IMCL CH₃/Cr. Correlations in the TA (black diamonds; Pearson's $r = 0.58$, $p = 0.005$, $n = 22$) and SOL (grey circles; $r = 0.67$, $p = 0.002$, $n = 19$) muscles, and TA and SOL together ($r = 0.52$, $p < 0.001$, $n = 41$). Decreases in the compositional marker (Δ CH₃:CH₂) are associated with decreases in Δ CH₃/Cr i.e. where there is net efflux (as Δ CH₃/Cr reflects net flux). (C) IMCL CH₂/Cr relative to CH₃/Cr at baseline reveals differences in IMCL CH₃:CH₂ ratio between TA (black diamonds) and SOL (grey circles) muscles ($p < 0.001$; paired samples t-test; $n = 19$).

compartments, with the exception of the cod liver oil where the tissue roll was olive oil. Three ¹H MR spectra were acquired from each phantom using the Point Resolved Spectroscopy sequence with the short echo time (TE) of 35 ms.

Participants and protocol. 24 healthy non-obese Caucasian male volunteers were recruited, aged 18 to 50 years without diabetes and taking no medication²⁸. They were asked to refrain from alcohol and vigorous physical activity and to follow their normal diet for 3 days prior to the study. Their meal on the evening prior to the study

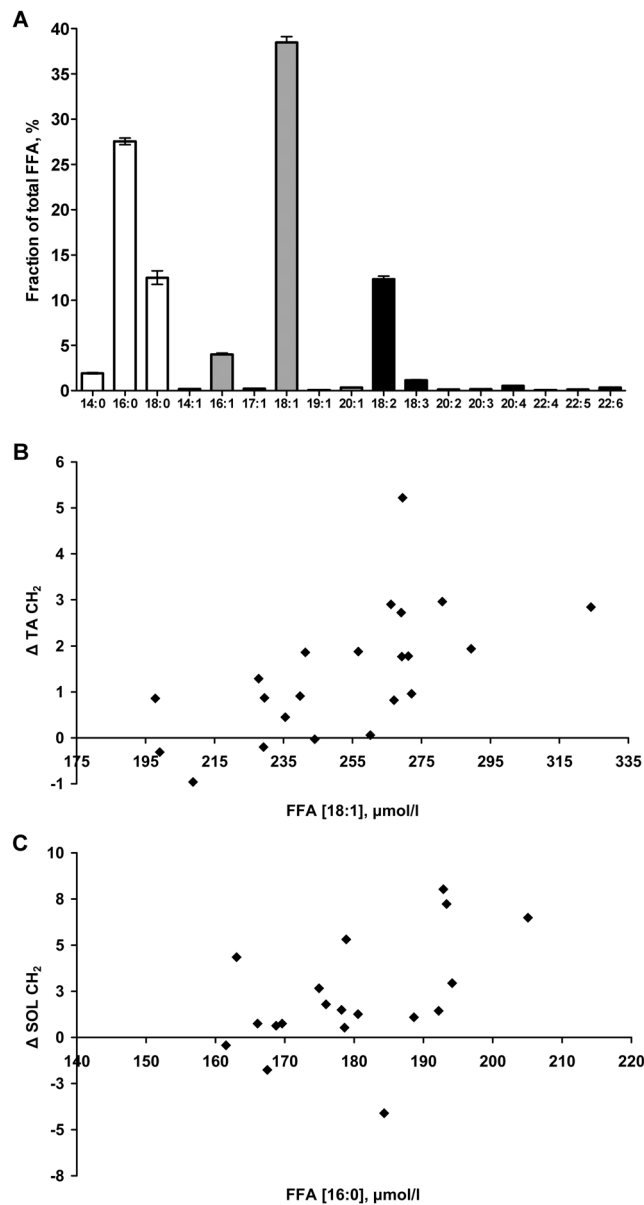


Figure 3. Circulating free fatty acids (FFA) ($\mu\text{mol/l}$, AUC) analysis after 12, 16 and 24 h fasting, and their relationship with the difference (Δ) in muscle IMCL CH₂ between 8 and 28 h fasting. **(A)** FFA profile (mean \pm SEM): total saturated FFA (white bars) constitute $41.9 \pm 1.0\%$, total monounsaturated (grey bars) $43.3 \pm 0.8\%$, total polyunsaturated (black bars) $14.8 \pm 0.4\%$, and total omega-3 (18:3, 22:5, 22:6) $1.62 \pm 0.06\%$ of total FFA. **(B)** and **(C)** show correlations: TA $\Delta\text{IMCL CH}_2$ ($n = 22$) was significantly correlated with concentrations of total monounsaturated (Pearson's $r = 0.60$, $p = 0.003$) FFA and specifically 18:1 ($r = 0.64$, $p = 0.002$) (shown in **B**), as well as total omega-3 FFA ($r = 0.43$, $p = 0.046$) with a tendency for total polyunsaturated FFA ($r = 0.41$, $p = 0.06$). In contrast SOL $\Delta\text{IMCL CH}_2$ ($n = 19$) correlated with combined saturated 14:0 + 16:0 ($r = 0.52$, $p = 0.02$) and 16:0 FFA alone ($r = 0.49$, $p = 0.03$) (shown in **C**).

(at 19:30) and following breakfast on day 1 (at 07:30) were standardized based on one-third of the recommended daily intake of energy and contained approximately 50% carbohydrate, 30% fat, and 20% protein. The study protocol involved fasting from 08:00 on day 1 to 14:00 on day 2. Magnetic resonance evaluations were undertaken at 8 and 28 h of fasting (16:00 on day 1 and noon on day 2) on a whole-body Siemens 3 T Verio scanner (Erlangen, Germany), with the voxels/slices being carefully relocalised on the second visit. Overnight blood samples for FFA assessment using high resolution mass spectrometry were taken at 20:00 (Day 1), 00:00 and 08:00 (Day 2).

Intramyocellular lipid (IMCL). Participants were placed supine and the peripheral-angio coil used for signal reception. A water-suppressed proton spectrum was acquired from a voxel of cube length 1.3 cm positioned to avoid visible fat on T₁-weighted images within TA and SOL, using acquisition parameters as in the phantom validation (TE = 35 ms, 5 s repetition time, and 64 averages). Phantom and *in vivo* data were analysed in jMRUI^{29,30}

and fitted with the AMARES³¹ algorithm using identical prior knowledge parameters: a single EMCL resonance, Gaussian lineshapes, soft constraints on EMCL/IMCL CH₂ frequencies and linewidths, CH₃ resonant frequencies and linewidths determined from known and inferred prior knowledge relative to the CH₂ resonance⁵, and with all amplitudes estimated. IMCL CH₂ and CH₃ are expressed relative to the creatine and phosphocreatine CH₃ resonance at 3.0 ppm.

Free Fatty Acids (FFA). Plasma samples were extracted with MTBE using an automated liquid handler. This organic phase was diluted with a mixture of isopropanol/methanol with 7.5 mM NH₄Ac solution. Lipid profiling was performed on the extract using chip-based nano-electrospray with an Advion TriVersa Nanomate (Advion, Ithaca, USA) interfaced to the Thermo Exactive Orbitrap (Thermo Scientific, Hemel Hempstead, UK), using a mass acquisition window from 200 to 2000 m/z and acquisition in positive and negative mode, as described elsewhere³². Negative mode data were used to measure relative concentrations of free fatty acids (FFA), and absolute FFA concentrations were calculated by comparison to the added internal standard undecanoic acid. Circulating FFA composition was reported from plasma samples at 12, 16 and 24 h fast, combined as the AUC.

Adipose tissue. Abdominal subcutaneous (SCAT_{abd}) and visceral (VAT) adipose tissue volumes were measured using magnetic resonance imaging over 6 cm superior-inferior distance from 5 water-suppressed T₁-weighted transaxial slices above the L5 vertebral level. Due to the higher reproducibility of leg subcutaneous adipose tissue (SCAT_{leg}) and intermuscular fat (IMF) (2 or 3% CoVs), these measures were assessed from a single T₁-weighted transaxial slice central to the ¹H MRS voxels, and hence these measures have units of area (cm²). Regional MRI analysis was performed in Analyze (AnalyzeDirect, Overland Park, KS).

Intrahepatic lipid (IHL). IHL was measured by ¹H MRS as previously described³³, and expressed as the methylene peak at 1.3 ppm relative to the water peak.

Statistics. All statistical tests were performed in IBM SPSS Statistics 23 (IBM, Armonk, NY: IBM Corp.), with significance set at P < 0.05. Normality was assessed by the Shapiro-Wilk test and non-normally distributed data were log-transformed prior to statistical testing. A 2-tailed paired-samples t-test was used to compare differences between 8 h and 28 h of fasting and Pearson's correlation coefficient for analyzing relations. Data are mean ± SEM.

Study approval. The study was approved by the Cambridge Local Research Ethics Committee and conducted in accordance with the Declaration of Helsinki. All participants provided written informed consent.

Data Availability. The datasets generated during the current study are available from the corresponding author on reasonable request.

References

- Meex, R. C. R., Schrauwen, P. & Hesselink, M. K. C. Modulation of myocellular fat stores: lipid droplet dynamics in health and disease. *Am J Physiol Regul Integr Comp Physiol* **297**, 913–924 (2009).
- Muoio, D. M. Revisiting the connection between intramyocellular lipids and insulin resistance: a long and winding road. *Diabetologia* **55**, 2551–2554 (2012).
- Machann, J., Haring, H., Schick, F. & Stumvoll, M. Intramyocellular lipids and insulin resistance. *Diabetes, Obes. Metab.* **6**, 239–248 (2004).
- Schrauwen-Hinderling, V. B., Hesselink, M. K. C., Schrauwen, P. & Kooi, M. E. Intramyocellular lipid content in human skeletal muscle. *Obesity* **14**, 357–367 (2006).
- Boesch, C., Machann, J., Vermathen, P. & Schick, F. Role of proton MR for the study of muscle lipid metabolism. *NMR Biomed.* **19**, 968–988 (2006).
- Goodpaster, B. H., He, J., Watkins, S. & Kelley, D. E. Skeletal muscle lipid content and insulin resistance: evidence for a paradox in endurance-trained athletes. *J Clin Endocrinol Metab.* **86**, 5755–5816 (2001).
- Stannard, S. R. *et al.* Fasting for 72 h increases intramyocellular lipid content in nondiabetic, physically fit men. *Am J Physiol Endocrinol Metab* **283**, E1185–91 (2002).
- Wietek, B. M. *et al.* Muscle type dependent increase in intramyocellular lipids during prolonged fasting of human subjects: A proton MRS study. *Horm. Metab. Res.* **36**, 639–644 (2004).
- Neumann-haefelin, C. *et al.* Lipid metabolism during starvation in Wistar rats. *Diabetes* **53**, 528–534 (2004).
- De Feyter, H. M. M. L. *et al.* Regional variations in intramyocellular lipid concentration correlate with muscle fiber type distribution in rat tibialis anterior muscle. *Magn. Reson. Med.* **56**, 19–25 (2006).
- Beha, A. *et al.* Muscle type-specific fatty acid metabolism in insulin resistance: an integrated *in vivo* study in Zucker diabetic fatty rats. *Am J Physiol Endocrinol Metab* **290**, 989–997 (2006).
- Halliwel, K. J., Fielding, B. A., Samra, J. S., Humphreys, S. M. & Frayn, K. N. Release of individual fatty acids from human adipose tissue *in vivo* after an overnight fast. *J. Lipid Res.* **37**, 1842–8 (1996).
- Price, E. R. & Valencak, T. G. Changes in fatty acid composition during starvation in vertebrates: mechanisms and questions. In *Comparative physiology of fasting, starvation, and food limitation* 237–255, https://doi.org/10.1007/978-3-642-29056-5_15 (Springer Berlin Heidelberg 2012).
- Herzberg, G. R. & Farrell, B. Fasting-induced, selective loss of fatty acids from muscle triacylglycerols. *Nutr. Res.* **23**, 205–213 (2003).
- Raclot, T. Selective mobilization of fatty acids from adipose tissue triacylglycerols. *Prog. Lipid Res.* **42**, 257–288 (2003).
- Schick, F. *et al.* Comparison of localized proton NMR signals of skeletal muscle and fat tissue *in vivo*: two lipid compartments in muscle tissue. *Magn. Reson. Med.* **29**, 158–167 (1993).
- Boesch, C., Slotboom, J., Hoppeler, H. & Kreis, R. *In vivo* determination of intra-myocellular lipids in human muscle by means of localized ¹H-MR-spectroscopy. *Magn. Reson. Med.* **37**, 484–493 (1997).
- Szczepaniak, L. S. *et al.* Measurement of intracellular triglyceride stores by ¹H spectroscopy: validation *in vivo*. *Am. J. Physiol. - Endocrinol. Metab.* **276**, E977–E989 (1999).
- Ren, J., Sherry, A. D. & Malloy, C. R. ¹H-MRS of intramyocellular lipids in soleus muscle at 7 T: Spectral simplification by using long echo times without water suppression. *Magn. Reson. Med.* **64**, 662–671 (2010).
- Škoch, A. *et al.* Intramyocellular lipid quantification from ¹H long echo time spectra at 1.5 and 3 T by means of the LCMoDel technique. *J. Magn. Reson. Imaging* **23**, 728–735 (2006).

21. Andersson, A., Nälsén, C., Tengblad, S. & Vessby, B. Fatty acid composition of skeletal muscle reflects dietary fat composition in humans. *Am. J. Clin. Nutr.* **76**, 1222–9 (2002).
22. Koutsari, C. & Jensen, M. D. Thematic review series: patient-oriented research. Free fatty acid metabolism in human obesity. *J. Lipid Res.* **47**, 1643–50 (2006).
23. Thamer, C. *et al.* Intramyocellular lipids: anthropometric determinants and relationships with maximal aerobic capacity and insulin sensitivity. *J. Clin. Endocrinol. Metab.* **88**, 1785–1791 (2003).
24. Hodson, L., Skeaff, C. M. & Fielding, B. A. Fatty acid composition of adipose tissue and blood in humans and its use as a biomarker of dietary intake. *Prog. Lipid Res.* **47**, 348–380 (2008).
25. DeLany, J. P., Windhauser, M. M., Champagne, C. M. & Bray, G. A. Differential oxidation of individual dietary fatty acids in humans. *Am. J. Clin. Nutr.* **72**, 905–11 (2000).
26. Lindeboom, L. & de Graaf, R. A. Measurement of lipid composition in human skeletal muscle and adipose tissue with ¹H-MRS homonuclear spectral editing. *Magn Reson Med* doi:10.100 (2017).
27. Guo, Z., Burguera, B. & Jensen, M. D. Kinetics of intramuscular triglyceride fatty acids in exercising humans. *J. Appl. Physiol.* **89**, 2057–64 (2000).
28. Thankamony, A. *et al.* Low circulating levels of IGF-1 in healthy adults are associated with reduced β -cell function, increased intramyocellular lipid, and enhanced fat utilization during fasting. *J. Clin. Endocrinol. Metab.* **99**, 2198–2207 (2014).
29. Naressi, A. *et al.* Java-based graphical user interface for the MRUI quantitation package. *Magma Magn. Reson. Mater. Physics, Biol. Med.* **12**, 141–152 (2001).
30. Stefan, D. *et al.* Quantitation of magnetic resonance spectroscopy signals: the jMRUI software package. *Meas. Sci. Technol.* **20**, 104035 (2009).
31. Vanhamme, L., Van Den Boogaart, A. & Huffel, S. Van. Improved method for accurate and efficient quantification of MRS data with use of prior knowledge. *J. Magn. Reson.* **129**, 35–43 (1997).
32. Eiden, M. *et al.* Mechanistic insights revealed by lipid profiling in monogenic insulin resistance syndromes. *Genome Med.* **7**, 63 (2015).
33. Semple, R. K. *et al.* Postreceptor insulin resistance contributes to human dyslipidemia and hepatic steatosis. *J. Clin. Invest.* **119**, 315–322 (2009).
34. Ren, J., Dean Sherry, A. & Malloy, C. R. Reply to: Intramyocellular lipids vs. intramyocellular triglycerides. *Magn. Reson. Med.* **67**, 299–299 (2012).

Acknowledgements

We thank the participants, staff at the Cambridge NIHR/Wellcome Trust Clinical Research Facility and the Wolfson Brain Imaging Centre, Sarah Nutland (NIHR Cambridge BioResource, Cambridge, UK) for facilitating participant recruitment and Edwina French (MRC Laboratory of Molecular Biology, Cambridge, UK) for help with phantoms. We acknowledge grants from Addenbrooke's Charitable Trust and the British Society for Pediatric Endocrinology and Diabetes. LH is a British Heart Foundation Senior Fellow in Basic Science. DBS is supported by the Wellcome Trust (107064). AT, AK and DBD are funded by the UK NIHR Cambridge Biomedical Research Centre and Medical Research Council (UD99999906), and AS by the NIHR via the NIHR Cambridge Clinical Research Facility.

Author Contributions

A.S. conceived the idea. A.S. undertook the phantom studies; A.T. and D.B.D. the fasting studies. A.K., V.B., C.B. and A.S. analyzed the data and A.T., G.J.K., A.K., C.B., L.H. and A.S. developed the interpretation. The manuscript was drafted by A.S., revised by G.J.K. and A.S., and then edited by all.

Additional Information

Competing Interests: The authors declare no competing interests.

Publisher's note: Springer Nature remains neutral with regard to jurisdictional claims in published maps and institutional affiliations.



Open Access This article is licensed under a Creative Commons Attribution 4.0 International License, which permits use, sharing, adaptation, distribution and reproduction in any medium or format, as long as you give appropriate credit to the original author(s) and the source, provide a link to the Creative Commons license, and indicate if changes were made. The images or other third party material in this article are included in the article's Creative Commons license, unless indicated otherwise in a credit line to the material. If material is not included in the article's Creative Commons license and your intended use is not permitted by statutory regulation or exceeds the permitted use, you will need to obtain permission directly from the copyright holder. To view a copy of this license, visit <http://creativecommons.org/licenses/by/4.0/>.

© The Author(s) 2018